Proc. Natl. Acad. Sci. USA
Vol. 95, pp. 13260–13265, October 1998
Neurobiology

Patch-clamp and amperometric recordings from norepinephrine transporters: Channel activity and voltage-dependent uptake

AURELIO GALLI, RANDY D. BLAKELY, AND LOUIS J. DEFELICE*

Department of Pharmacology and Center for Molecular Neuroscience, Vanderbilt University Medical Center, Nashville TN 37232-6600

Edited by Charles F. Stevens, The Salk Institute for Biological Studies, LaJolla, CA, and approved August 13, 1998 (received for review June 15, 1998)

ABSTRACT **Transporters for the biogenic amines dopamine, norepinephrine, epinephrine and serotonin are largely responsible for transmitter inactivation after release. They also serve as high-affinity targets for a number of clinically relevant psychoactive agents, including antidepressants, cocaine, and amphetamines. Despite their prominent role in neurotransmitter inactivation and drug responses, we lack a clear understanding of the permeation pathway or regulation mechanisms at the single transporter level. The resolution of radiotracer-based flux techniques limits the opportunities to dissect these problems. Here we combine patch-clamp recording techniques with microamperometry to record the transporter-mediated flux of norepinephrine across isolated membrane patches. These data reveal voltage-dependent norepinephrine flux that correlates temporally with antidepressant-sensitive transporter currents in the same patch. Furthermore, we resolve unitary flux events linked with bursts of transporter channel openings. These findings indicate that norepinephrine transporters are capable of transporting neurotransmitter across the membrane in discrete shots containing hundreds of molecules. Amperometry is used widely to study neurotransmitter distribution and kinetics in the nervous system and to detect transmitter release during vesicular exocytosis. Of interest regarding the present application is the use of amperometry on inside-out patches with synchronous recording of flux and current. Thus, our results further demonstrate a powerful method to assess transporter function and regulation.**

Transporter-mediated clearance of neurotransmitters after vesicular release represents a crucial mechanism for temporal and spatial regulation of chemical signaling (1–5). Transporters for the biogenic amines dopamine, norepinephrine (NE), and serotonin (5HT) have particular significance as targets for clinically relevant psychoactive agents including, cocaine, antidepressants, and amphetamines (6). Cocaine and antidepressants are transporter antagonists that act with varying degrees of specificity to enhance synaptic concentrations of amines by limiting clearance (2, 6–8). Amphetamines enhance transporter mediated efflux in concert with a depletion of vesicular amine stores (8, 9). The localization of cocaine and antidepressant-sensitive transporters to the presynaptic neuron extends their influence to homeostatic relationships for transmitter biosynthesis and release.

To date, the mechanisms of plasma membrane amine transport have been inferred primarily through transmitter-based flux measurements on populations of cells of isolated membrane fractions (10, 11). These assays predict the transport of amines to be coupled energetically to the inward movement of Na and Cl ions. In the case of 5HT transporters, this flux is coupled to the counter transport of K ions (11, 12), rendering 5HT transporters theoretically electroneutral. In the case of the NE transporter, the coupling stoichiometry predicted from cell and membrane vesicle flux studies is 1NE:1Na:1Cl, which implies a net charge transfer of 1 electronic charge unit per turnover cycle. For a turnover rate of 1/sec, the predicted average current is insignificant even with high expression (<0.1 pA for 10^6 transporters). Biophysical studies have, however, revealed addition properties of transporters that support the existence of large currents during the ion channel mode of conduction (13, 14). These currents are gated by transmitter, blocked by transporter antagonists, and absent from nonexpressing cells (13–20). Furthermore, we recently have identified transporter-associated channel activity in cell-detached patches of NE transporter (NET)-expressing cells (21). These later studies suggest new opportunities to study transporter mechanisms. At the same time, they challenge simple alternating access models to explain transporter behavior completely. Previously, we were unable to measure simultaneously transporter currents and amine transport across small patches that showed single transporter activity. Therefore, our observations could be explained by NE-induced channel activity unrelated to amine movement, thus clouding opportunities to clarify transporter mechanism and regulation at the single transporter level. For example, recent studies of PKC-dependent dopamine and 5HT transporter regulation demonstrate a loss of amine transporter currents in single cells that accompanies a loss of transporter from the cell surface (22, 23). It is therefore difficult to evaluate whether the loss of current and surface protein represents the same event or separate stages in an unresolved regulatory process. Such questions will remain unanswered until we measure transmitter flux with a time resolution comparable to transporter currents.

Microamperometry, which relies on the oxidation of catecholamines, can detect small quantities of neurotransmitter released during vesicular exocytosis (24–26). Amperometry also has a long history in the distribution and kinetics of neurotransmitters in the nervous system (refs. 27–30; http://biosci.umn.edu/biophys/OLTB/Textbook.html). Of interest regarding the present application is the use of amperometry on inside-out patches with synchronous recording of flux and current. We determined that these techniques were sufficiently sensitive to report transporter-mediated NE flux in transporter-dense patches pulled from NET-transfected cells. Here, we describe simultaneous recordings of NET-associated currents and NET-facilitated NE flux. We establish that microamperometry can detect small NE movements across NET-expressing patches that depend on extracellular Na and Cl ions. These NE fluxes are absent in patches from nonexpressing cells and are blocked by multiple NET-specific antagonists. Our studies further reveal a significant temporal correlation between transporter channel behavior and NE flux and demonstrate directly the influence of membrane potential on NE flux and stoichiometry. Moreover, we resolve rapid, antidepressant-sensitive transits of NE that are linked to ion flow. These data suggest that NETs can mediate a

The publication costs of this article were defrayed in part by page charge payment. This article must therefore be hereby marked "*advertisement*" in accordance with 18 U.S.C. §1734 solely to indicate this fact.

This paper was submitted directly (Track II) to the *Proceedings* office.

Abbreviations: NE, norepinephrine; NET, NE transporter; hNET, human NET; DS, desipramine; e, electron.

A Commentary on this article begins on page 12737.

*To whom reprint requests should be addressed. e-mail: lou.defelice@mcmail.vanderbilt.edu.

form of substrate permeation in which transmitter can move across the membrane in shots in an open-channel mode. These experiments, therefore, indicate a channel mechanism for neurotransmitter uptake, and they present a method to assess transporter function and regulation.

METHODS

Generation of the Stably Transfected Cell Lines. To relate current and uptake, we used inside-out patches removed from HEK-293 cells stably transfected with human NETs (hNETs). An *Xho*I/*Xba*I fragment containing cDNA for hNET was cut from pBluescript SKII- and was subcloned into *Xho*I/*Xba*I-digested pcDNA3 (Invitrogen), placing control of hNET expression under CMV and T7 RNA polymerase promoter. To generate stable lines, we transfected hNET/pcDNA3 by using Lipofectin (Life Technologies, Grand Island, NY). We plated cells at 60% confluence in DMEM with 10% heat-inactivated fetal bovine serum, 100 μg/ml penicillin, and 100 units/ml streptomycin. After 3 days, we switched cells to a medium containing 250 μg/ml geneticin (G418) and isolated resistant colonies 1 week later. We used single cells to generate the clonal lines, testing multiple lines for desipramine-sensitive [^{3}H]NE uptake. Line 293-hNET-#3 was used in all our experiments.

Electrophysiology. A voltage-clamped pipette (patch electrode) filled with an external solution plus NE monitored the desipramine (DS)-sensitive channel activity (21). Before recording from parental or stably transfected cells, they were plated at 10^5 per 35-mm culture dish. Attached cells were washed three times with bath solution at 37°C. In Fig. 1*A*, the top electrode is in the cell-detached configuration, with the inner membrane exposed to the perfusion solution (130 mM KCl/0.1 mM $CaCl_2$/2 mM $MgCl_2$/1.1 mM EGTA/10 mM Hepes/30 mM dextrose, adjusted to pH 7.35; free Ca was 0.1 μM). In the inside-out orientation, a positive potential applied to the pipette corresponds to a hyperpolarization of the membrane. (Note that −100 mV in Fig. 1*A* indicates the normal sign convention, as experienced by the membrane, not the voltage actually applied to the interior of the pipette). Similarly, current flowing out of the pipette indicates an inward current. The inside-out patch was held 1 to 2 μm from the carbon fiber, which itself was held at +700 mV for NE oxidation (25, 31–33). Although we tried touching the fiber to the membrane, as done in other preparations, for cell-detached patches this proved extremely unfavorable for the stability of the patch. The patch electrode contained an external-like solution (130 mM NaCl/1.3 mM KCl/1.3 mM KH_2PO_4/0.5 mM $MgSO_2$/1.5 mM $CaCl_2$/10 mM Hepes/34 mM dextrose) plus 4 mM NE. We use 4 mM NE because this is a reserve against unwanted oxidation in the pipette and because higher concentrations increase hNET permeability to NE, thus facilitating the measurement. It is also significant that 4 mM NE may mimic the concentration in the synaptic cleft. In the ion replacement experiments, N-methyl-D-glucamine totally substituted for Na. Instead, Cl was replaced only partially with acetate, retaining 1.5 mM Cl in the pipette solution. Unwanted offsets and extraneous noise were lessened by using a mini-agar salt bridge containing normal Cl concentration. We attached this bridge to the Ag/AgCl wire in the patch electrode.

Patch electrodes (≈5 MΩ when filled with the pipette solution and dipped into the intracellular bath solution) were pulled from quartz pipettes on a P-2000 puller (Sutter Instruments, Novato, CA). Data were recorded on a VCR and were analyzed off-line. We used an Axopatch 200-A (Axon Instruments, Foster City, CA) voltage-to-current converter (with a low-pass frequency window in series with the 200 A defined by a 4-pole Butterworth filter set at 5,000 Hz) to record current through the inside-out patch. Voltage steps (2 sec) ranging from −100 to +60 mV were separated by 0-mV holding potentials (4 sec). We used an Axopatch 200B voltage-to-current converter (low-pass 4-pole Butterworth filter set at 1,000 Hz) to record the oxidative (amperometric) current. This second amplifier held the fiber at +700 mV for all experiments unless noted otherwise. Note that both amplifiers share a common ground; thus, it is the working fiber itself that is held at the oxidation voltage, not the bath (http://biosci.umn.edu/biophys/OLTB/Textbook.html). We obtained the carbon fiber electrodes (ProCFE; fiber diameter is

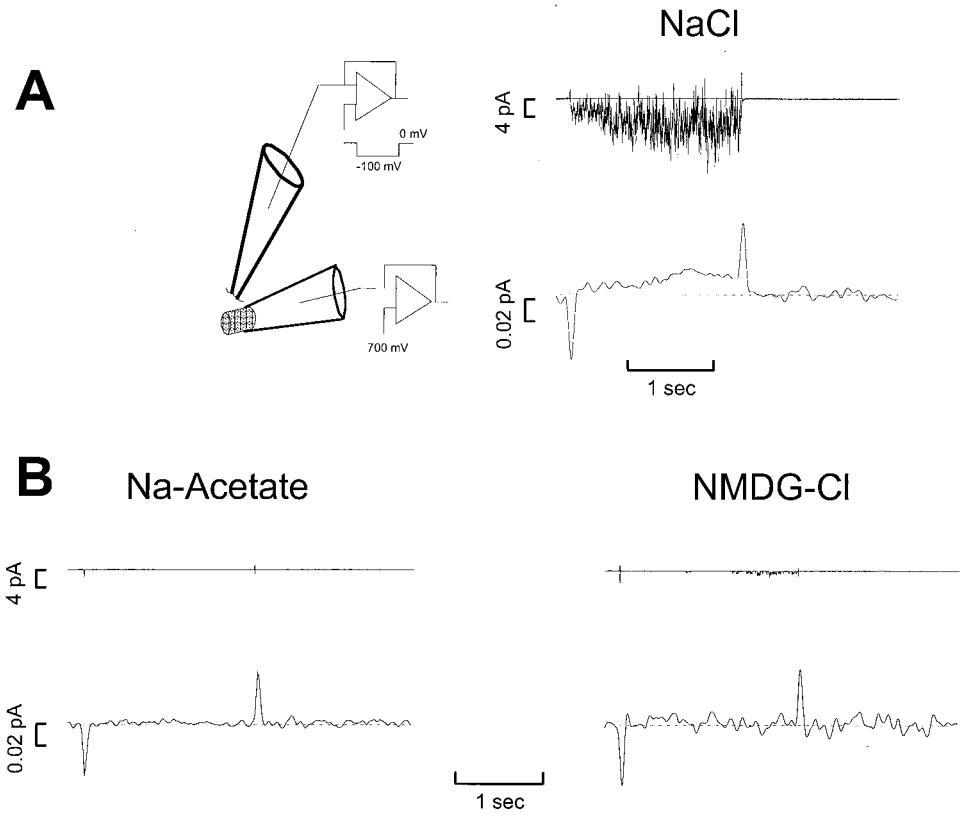

FIG. 1. *A* (left) is a diagram of the experimental setup. The top electrode forms an inside-out patch from hNET-transfected HEK-293 cells that is voltage clamped to 0 mV for 4 sec and to −100 mV for 2 sec. The bottom amperometric electrode holds a carbon fiber held +700 mV. All experiments were done at 37°C. *A* (right) shows typical recordings from a patch electrode (containing an external-like solution plus 4 mM NE) and an amperometric electrode. *B* (left) shows an experiment similar to *A* except that the patch pipette contains Na acetate in place of NaCl. The response in the patch and in the amperometric electrode is null. *B* (right) shows an experiment similar to *A* except that N-methyl-D-glucamine replaces Na as the major cation in the pipette. From these experiments, the response in the amperometric electrode that correlates with the patch current depends on the presence of Cl and Na. To control for the possibility that the patches used in these controls may contain low numbers of transporters, we repeated this experiment with 14 patches without Cl and 11 patches without Na, with the same result.

5 μm) from Axon instruments. Traces were filtered for analysis/ as noted.

Amperometry. A carbon fiber (amperometric electrode) measures the NE flux (31). DS is a specific blocker that reduces NE uptake in native and NET-transfected tissue (34), and DS specifically abates NE uptake and NE-induced currents in hNET-transfected HEK-293 cells (14). We step the voltage for 2 sec to test voltages and record the patch current and the oxidative current simultaneously. At the holding potential of 0 mV there is an apparent flux of NE from the patch, as indicated by the downward deflection at positive voltages (Fig. 2). The downward deflection saturates at +60 mV, making it a convenient reference point for each patch and consistent with evidence (35) that uptake approaches zero at positive potentials. This procedure constitutes an internal calibration for each electrode. Unlike the usual amperometric calibration, which requires conversion to concentration, we report the current directly without considering the effective volume. Thus, our requirements are a defined baseline, and our data represent a lower limit to the NE flux because some transmitter is lost to the bulk solution. The relationship between the oxidative current and the number of NE molecules reacted is given by Faraday's law: $Q = zeM$, where Q is the total charge involved in the redox reaction, M is the number of molecules reacted, and z is the number of electronic charges (e) transferred per reacted molecule. The number of electrons that NE can contribute is a time-dependent oxidation process (33). Thus, to calculate the number of NE molecules reacted with the carbon fiber, we used $z = 3$ for 2 sec pulses and $z = 2$ for short bursts (<0.2 sec). Patch currents and amperometric currents were low pass filtered at 1 kHz and 5–50 Hz, respectively.

Data Analysis. The correlation coefficient is a rescaling of the covariance, S_{XY}, of X and Y by the standard deviation of X and Y: thus, $R = S_{XY}/S_X S_Y$ has a value between −1 and 1 (36). Because the patch current is the total current, R is affected by the number and type of non-hNET-associated currents present in the detached patch. The oval data points are used to indicate a larger absolute total patch current (I_{TOT}) scale compared with the NE oxidation current (I_{AMP}).

RESULTS AND DISCUSSION

NE Oxidation Current Depends on Na and Cl. Fig. 1 illustrates the method used to measure the transporter-associated current and the transmitter transport simultaneously. The method uses conventional patch-clamp techniques combined with microamperometry. We first form an inside-out patch from a hNET-transfected HEK-293 cell and apply step pulses to the membrane. Then, we place a carbon fiber under the patch and clamp it to +700 mV (or other voltages as indicated). In Fig. 1*A*, the patch pipette contains normal physiological saline plus 4 mM NE. With NE in the pipette, this protocol results in inward currents that are blocked by the NET-specific antagonists DS and nisoxetine (6, 34, 37). In patches that contain few transporters, the DS-sensitive currents appear as channel-like events (21). In patches that contain many transporters, as in Fig. 1, the individual events are not resolved. The DS-sensitive currents are paralleled by an oxidative current in the amperometric electrode. The oxidative current is absent if the patch electrode contains no NE or if the patch came from nontransfected cells. Moving the carbon fiber away from the patch causes the oxidative response to become smaller and slower. Finally, as expected for NE oxidation (31–33),

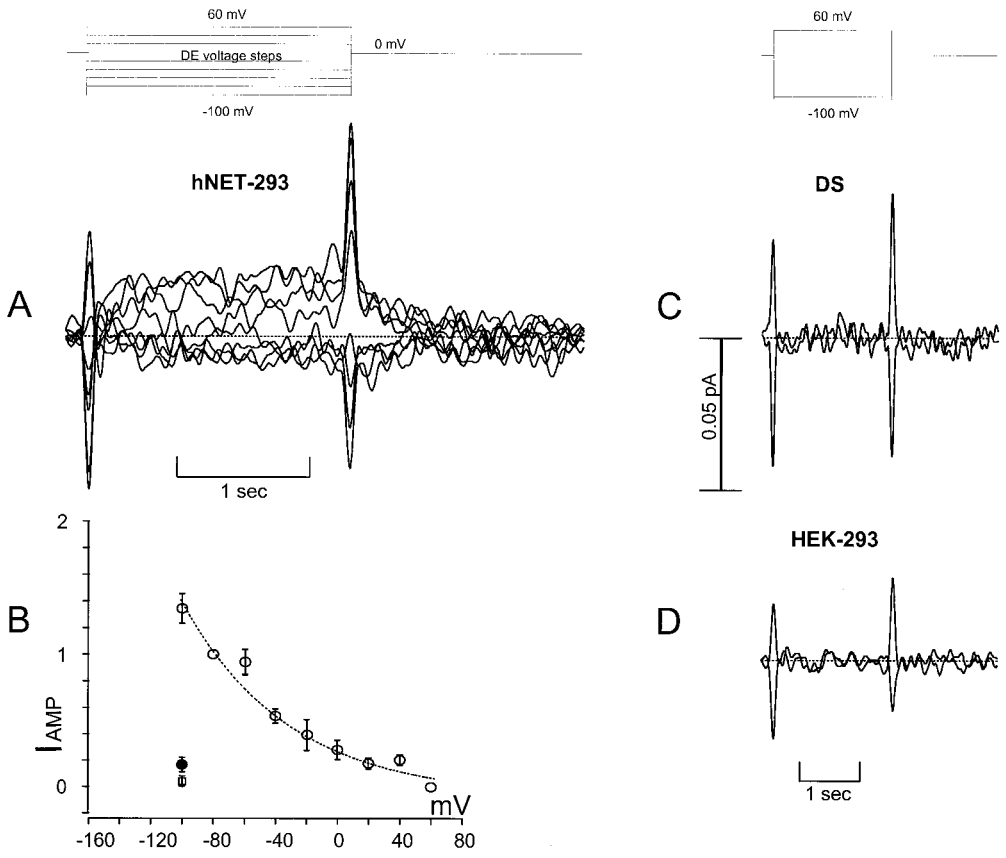

FIG. 2. *A* shows raw oxidative currents as a function of voltage. The amperometric traces were low-pass filtered at 5 Hz. *A* shows that hyperpolarizing steps induced positive amperometric currents. An upward (positive) deflection indicates NE oxidation and thus represents movement of NE out of the patch in the direction of "uptake." At 0 mV there is uptake because depolarizing the patch caused a downward deflection (less NE being oxidized). The 0.05-pA scale applies to the entire figure; however, the 2-sec scale is expanded in *A*. Transient capacity current on the amperometric traces indicates the voltage step. The data points and bars indicate average ± SEM. *B* shows the steady-state amperometric current plotted against the patch-test voltage. The level of NE uptake indicated by the oxidative current increases at negative voltages without saturation in the range studied. In contrast, NE uptake saturates at positive voltages, and at 60 mV there was further deflection, consistent with previous data on voltage-dependent uptake. We therefore defined NE uptake (open circles) as the amperometric current at a particular voltage minus the current at 60 mV. To comparecells, data($n = 5$) are represented as the fraction of theamperometric current arbitrarily normalized at −80 mV. The dotted line represents a Marquardt nonlinear, least squares polynomial fit. Adding 12 μM DS to the bath at the maximal current re-duced NE uptake close to zero (filled circle, $n = 4$). We obtained a similar result with parental HEK-293 cells (open square, $n = 13$). *C* shows the effect of 12 μM DS added to the bath on amperometric currents recorded in hNET-293 cells at +60 and −100 mV (same cell as *A*; 4 mM NE in the patch pipette). *D* shows similar raw traces from patches removed from HEK-293 cells and clamped to +60 and −100 mV, with normal extracellular solution plus 4 mM NE in the pipette. The 4 mM NE response was blocked by 12 μM DS or 4 μM nisoxetine ($n = 3$) (data not shown), a more potent inhibitor of hNET.

the oxidative response diminished if we reduced the carbon fiber voltage to +300 mV and disappeared completely on further reduction. Fig. 1*B* illustrates that Cl and Na are essential to obtain the oxidative response. Thus, neither the DS-sensitive current nor the oxidation current is present if, in the patch-pipette, acetate replaces Cl or N-methyl-D-glucamine replaces Na. This is further evidence that the oxidative response is associated with hNETs because norepinephrine transport depends on the presence of these two ions (35, 38). These leak-subtracted controls also indicate that the oxidative response is not merely a nonspecific NE discharge through the seal or the patch. If the oxidation current were leakage, we would expect a response in the absence of Cl or Na, in the presence of DS or nisoxetine, or from patches removed from parental cells. In none of these cases do we observe NE oxidation currents. These results strongly suggest that the oxidation current results from NE moving through the patch via hNETs. Assuming that the oxidation of one NE molecule contributes three electrons per oxidation (28), the area of the oxidation current in Fig. 1*A* implies that 66,000 NE molecules pass through the patch during a 2-sec interval. This is an underestimate because not all NE molecules that exit the patch reach the fiber, and those that do are not necessarily oxidized. The number of NE molecules is variable from experiment to experiment and likely depends on the number of transporters in the patch. As shown below, however, the number of NE molecules that undergo oxidization correlates with the size of the DS-sensitive current.

NE Oxidation Current Increases with Hyperpolarization. Previous studies have indicated that NE uptake should increase at negative potentials (35, 39). However, the transport–voltage relationship and the mechanism of this dependence are unknown. Fig. 2*A* shows oxidation currents obtained at different patch voltages. By convention, oxidation current is plotted positive, and reduction current is plotted negative. In the inside-out orientation, recall that positive current flowing out of the patch to the bath indicates an inward current. In the amperometric electrode, an upward (oxidative) deflection corresponds to an inward current through the patch (NE moving into the bath). Therefore, positive oxidative current represents NE uptake. In Fig. 2*B*, we have plotted the mean value of the steady-state oxidation current (I_{AMP}) against the test voltage applied to the patch (Fig. 2*B*). The plot was normalized at −80 mV to facilitate comparison of patches. The figure shows that NE uptake increases at negative potentials. This is in qualitative agreement with previous investigations of monoamine transporters (19, 40). Fig. 2*B* shows that DS blocks the oxidative current in cells capable of generating amperometric current (solid circle, $n = 4$). DS-insensitive channels do not induce a corresponding response in the carbon fiber (not shown). Finally, we detect no response from parental HEK-293 cells (open square, $n = 13$). Fig. 2 *C* and *D* show raw traces from DS-treated transfected cells (showing oxidative currents before DS treatment) and from parental cells, which are virtually identical for 4 mM NE patches between −100 and +60 mV. These experiments provide strong evidence that the carbon fiber reports NE flux via hNET and that Fig. 1B is, therefore, the hNET uptake–voltage relationship.

NE Oxidation Current Relative to Total Current Decreases with Hyperpolarization. To quantify the relative NE oxidation current (I_{AMP}) to the total patch current (I_{TOT}) we calculated their ratio. In a separate set of experiments, Fig. 3 shows the average NE oxidative current during a 2-sec pulse (open circles), the average DS-sensitive patch current (closed squares) (21), and the ratio of these two currents (ρ) as a function of voltage (closed circles). The increase of I_{TOT} through the patch is similar to that observed in previous whole-cell studies (14). These data show in a direct and simultaneous measurement that the fraction of current carried through the transporter by NE (ρ) decreases at negative potentials. A voltage-dependent parameter analogous to ρ(V) was measured for dopamine (20) and serotonin (19) transporters. Although in these cases uptake and current were not

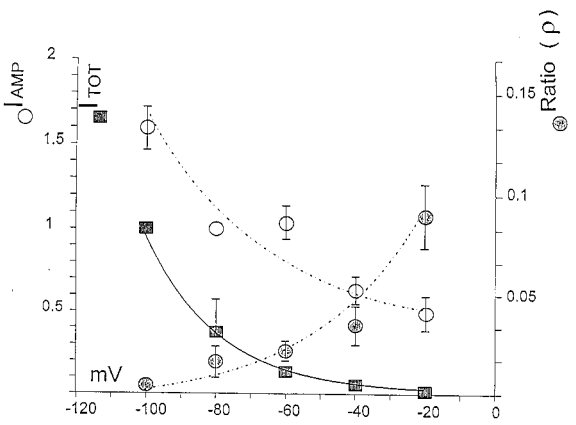

FIG. 3. The filled squares represent the average NE-induced current during 2-sec voltage steps (4 mM in the pipette, as in Fig. 1*A*). We define NE-induced current as the current during a protocol minus the unblocked current after adding 8–12 μM DS to the bath ($n = 3$). Data points and bars indicate average ± SEM. The open circles represent the average amperometric current during 2-sec voltage steps; we obtained these values by subtracting the average current at +60 mV from the current at each potential. To separate the two curves, we normalized the filled squares at −100 mV and the open circles at −80 mV. The filled circles are the ratio (ρ) of the average amperometric current to the DS-sensitive patch current. This ratio shows that the percentage of the current carried by NE increases with potential. By using $z = 3$ to convert I_{AMP} into NE molecules, the oxidation products during the 2-sec pulse, at −20 mV, NE carries more than nearly 10% of the NE-induced current. Although uptake increases at negative voltages (open circles), ρ values decrease because more total charge is translocated.

measured simultaneously, the trend for greater uptake at negative voltages is the same as in the present result. For hNET, NE carries 10% of the total current at −20 mV but <1% at −100 mV. Therefore, although transport increases with hyperpolarization, total current increases more. Because patches with different DS-sensitive currents have similar ρ at the same voltage, ρ is apparently independent of the number of transporters. Consequently, ρ(V) reflects the uptake-to-current ratio for individual transporters. This ratio, therefore, converts NE-induced current to NE transport independent of the number of transporters.

NE Oxidation Current and Total Current Are Correlated Temporally. Thus far, we have shown the quantitative relationship between the NE oxidation current and NE-induced current through hNETs. As pointed out, identical results could be obtained if transporters switched between alternating access and channel modes or if transport and channel modes were combined (16, 21). To test for a common pathway for NE and other ions, we evaluated the temporal relationship between I_{AMP} and I_{TOT}. Fig. 4*A* shows a parametric plot of the NE oxidation current and the total patch current for an experiment similar to Fig. 1*A*. The strong correlation between I_{AMP} and I_{TOT} (the correlation appears positive because we represented inward current as increasing from left to right). To compare many patches, we evaluated the average Pearson product moment (R) for I_{AMP} and I_{TOT} (see *Methods*). For four experiments, $R = 0.58 \pm 0.11$ (average ± SEM, $n = 4$). After adding 12 μM DS ($n = 4$) or 4 μM nisoxetine ($n = 3$), or after replacing Na with N-methyl-D-glucamine ($n = 11$) or Cl with acetate ($n = 14$), to within experimental error, $R = 0$. Patches from parental cells also have $R = 0$ ($n = 13$), as illustrated in Fig. 4*B*. The results indicate strong temporal correlation between the oxidative current and the NE-induced single-channel currents, suggesting that transport and channel openings occur at the same time. The channel mode and the transport mode could, however, be separate events that are linked kinetically by allosteric interactions. This also would lead to the observed correlation. Allosteric gating models have been proposed by others (15, 16). For example, it has been suggested (41, 42) that the γ-aminobutyric acid transporter GAT1 may act as a

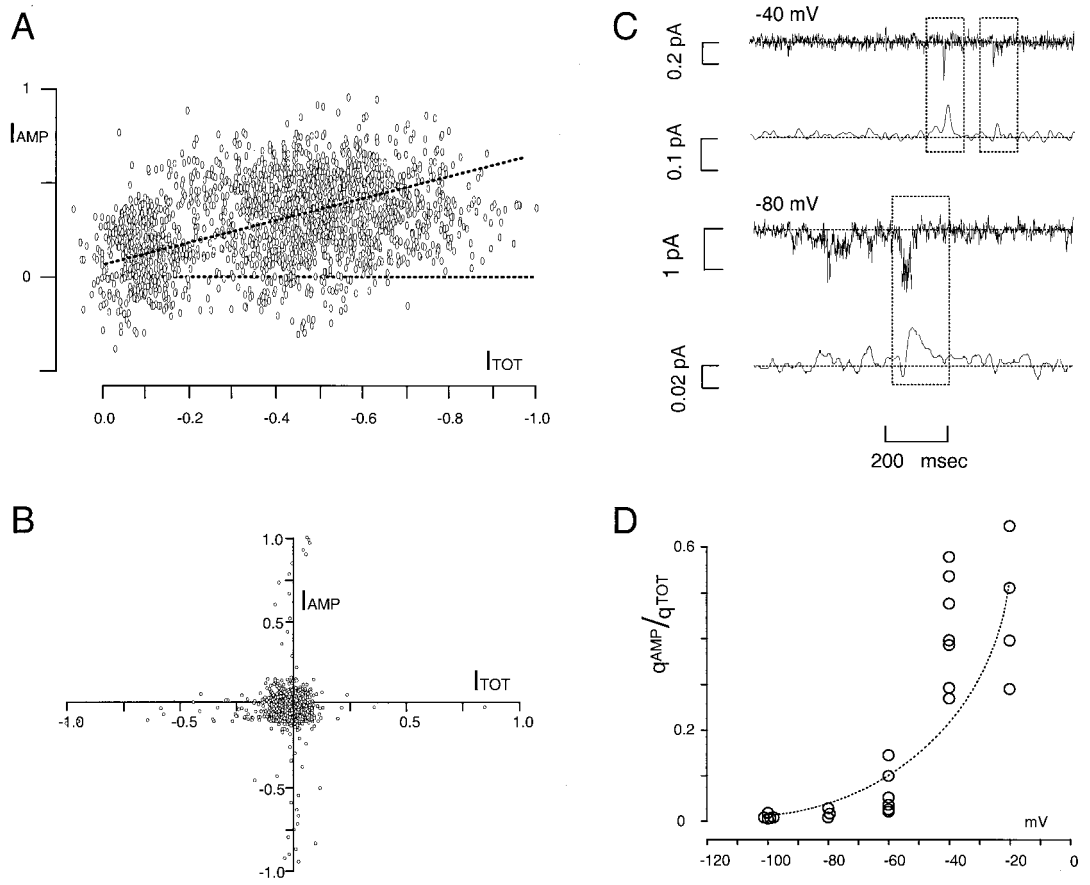

FIG. 4. *A* illustrates the correlation between NE-induced current through the patch and the NE released from the same patch (4 mM NE in the pipette; compare with raw data in Fig. 1). The illustrated data are from a patch stepped from 0 to −100 mV, and the plot is the normalized time-varying NE-induced current (I_{TOT}) against normalized time-varying NE-uptake (I_{AMP}). Both traces were low-pass filtered at 50 Hz. The slope of the point dispersion was evaluated by using the sample Pearson product moment (R). At −100 mV, where we record the strongest amperometric current, $R = 0.58$ (slanted dotted line). The flat line indicates zero correlation. *B* illustrates the time relation between patch and amperometric currents from a parental cell patch with 4 mM NE in the pipette; in these cases, R was zero in 13 experiments. Controls on transfected cells with no NE in the pipette or with 4 mM NE in the pipette but 12 μM DS or 4 μM nisoxetine in the bath gave similar negative results. *C* shows isolated NE-induced, DS-sensitive current events at −40 and −80 mV and simultaneous recordings from the amperometric electrode. The dotted rectangles focus attention on typical pairs selected for analysis. *D* shows the ratio (γ) of the amperometric charge, q_{AMP}, to the corresponding patch-current charge, q_{TOT} (data from seven different patches) as a function of patch voltage.

pore with allosteric ion gates. Our model differs from other models, however, in that we explicitly suggest transmitter and other ions can move through a common pathway in the channel mode.

To test for a common pathway, we selected patches with low hNET activity. In such patches, we compared discrete events in the patch with discrete time-correlated events in the carbon fiber. Individual transporter events are probably not observable by amperometry at present. Considering the transporter as a point source, a 5 μm diameter carbon fiber 2 μm from the transporter would only report events >3 msec in duration (43). Our data typically show amperometric events that average between 5 and 50 msec in duration. However, based on the size and duration of the concomitant current (21), the majority of pairs in all likelihood represent overlapping bursts of 3–10 transporters that could be flickering open rapidly or have multiple conducting states. Because of diffusional blurring, individual events, even if observed with perfect fidelity, might be much faster and have higher amplitude than the present recordings suggest.

Note, however, that, although individual channels may open with no apparent response in the carbon fiber, the reverse does not occur. Each oxidative response parallels a discrete patch event. Furthermore, the larger the patch current, the larger the oxidation current. Fig. 4*C* illustrates two different events at −40 mV for which the ratio of NE to total charge is the same (see below). Such pairs are absent in parental cells, and they are blocked after exposure to DS. The oxidative events that we were able to detect were on average between 5 and 50 msec in duration. The total charge (q_{TOT}) and the NE charge (q_{AMP}) are the areas under these currents. Fig. 4*C* illustrates a long event at −80 mV. The integrated patch current carries a net charge of 250,000 e and the accompanying oxidation current contains a net charge of 12,800 e (6,400 NE molecules, assuming two e per oxidation) (33). Such pairs are correlated strongly ($R = 0.9 \pm 0.05$ for $n = 25$). The criterion we used to define the integration is a standard deviation above the rms level defined for a period with no obvious events. These values were used to define the ratio $\gamma = q_{AMP}/q_{TOT}$ for pairs at different patch potentials (Fig. 4*D*). In agreement with patches that contained many channels (Fig. 3), hyperpolarization decreases the fraction of charge that NE carries through hNET. However, although ρ obtained from many transporters was 10% at −20 mV, the analogous γ values obtained from 3–10 transporters ranged between 30–60% at the same potential. A possible explanation is that the proportion of oxidized NE molecules changes for large signals or merely that we artificially select for large oxidative events in the microscopic experiments.

This paper documents the simultaneous, real-time measurements of voltage-dependent transmitter uptake. It further shows that NE flux is 100× more efficacious at −100 mV than at −20 mV. The implication is that noradrenergic synapses clear more rapidly at hyperpolarized potentials than at depolarized potentials. One prediction of these results is that the NE-induced current would depolarize the synaptic terminal, and thus transport would self-regulate downward during the early phase of transmitter release. Eventual repolarization would return the transporter to its maximum efficiency for maintaining extracellular NE at a low concentration. Regardless of this interpretation of voltage-dependent uptake, our results indicate an additional mechanism for uptake. Such a mechanism, however, may have limitations for uphill transport. Basal cytoplasmic concentration of catecholamines is 1–2 μM in pheochromocytoma cells or giant snail neurons (44, 45) whereas basal levels of extracellular catecholamines are typically 5–50 nM (46, 47). Because uncoupled mechanisms only support a 10:1 ratio at −60 mV, it is unlikely

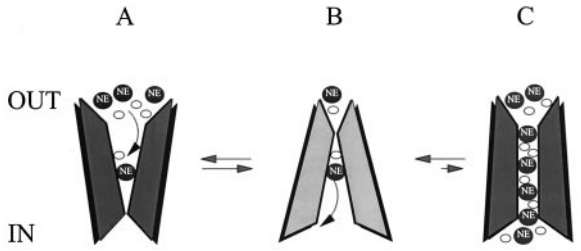

FIG. 5. Schematic of hNET carrier (alternating-access) and channel modes. The alternating access model assumes that a state transition for NE permeation ($A \leftrightarrow B$) results in the transport of a single NE molecule. The channel mode (C) is a low probability event that requires NE, Na, and Cl for activation. The amperometric spikes consist of hundreds of NE molecules crossing the membrane coupled with other ions down their electrochemical gradients.

that uncoupled mechanisms alone can account for the observed basal gradients. The temporal correlation between NE flux and NE-induced current may indicate that NE uptake detected with amperometry and channel activity in the patch membrane arise from the same kinetic process. This conclusion is strengthened by the observation of temporally correlated oxidative spikes with channel events and that microscopic $\gamma(V)$ and macroscopic $\rho(V)$ ratios have similar voltage-dependence. In such a model, NE, Na, and Cl would induce hNETs to transport in the carrier mode (Fig. 5 *A* and *B*) and occasionally would switch to a channel mode. Unlike other models, however, NE itself also could move through the channel down its electrochemical gradient (Fig. 5*C*). A channel that does not mediate transport cannot explain the present data because the amperometric spikes that correlate with channel activity contain thousands of NE molecules. If only one NE molecule were transported, we would be unable to detect an amperometric signal unless thousands of carriers acted simultaneously. This excludes the possibility that the temporal correlation merely results from a nontransmitter-conducting channel that opens during the transporter cycle. One prediction of the present model is that NE flux should be a complex function of NE concentration and voltage because NE acts both as a ligand and as a permeant ion. Previously, we have worked below 100 μM NE because K_{NE} is $\approx$0.6 μM for both NE-induced current and NE uptake (14, 21). Thus, all NE-induced channels are activated at low concentrations; however, the flux through an open channel sees the concentration of external NE as a driving force. Although the phenomena we report here are observable at concentrations as low as 100 μM, we used high concentrations of NE because this facilitated the amperometric measurement.

It is worth pointing out that millimolar concentrations also may mimic transient concentrations in the synaptic cleft. Electrochemical techniques similar to those used here indicate 170 to 500 mM serotonin or catecholamines in secretory vesicles (24–26). Furthermore, γ-aminobutyric acid, glutamate, and glycine concentrations peak at 1–5 mM concentrations in the synaptic cleft (48). Recently, it has been shown (30) that the concentration of 5HT in the cleft may reach levels as high as 6 mM. Transporters in transfected cells or resealed vesicles apparently saturate at concentrations in the micromolar range in which a carrier model explains the data. The NE conductance reported here is distinct from this stoichiometric transport and represents a channel mode of neurotransmitter transport. Our experiments do not, however, exclude stoichiometric uptake via a carrier because $\approx$1 NE/sec is far below our limit of resolution. At -60 mV, we have demonstrated that NE carries 2% of the transporter current and that this transport may occur at a rate of 30,000 NE/sec. It is possible that these bursts of NE transport represent 30,000 transporters acting simultaneously. However, judging from the amplitude and duration of the concurrent channel activity (21), these bursts of NE are composed at most of 3–10 transporters acting as channels. Thus, if NETs can transport transmitters via channels, the channel mechanism of NE transport may dominate during the early stages of transmitter clearance.

We thank Dawn Borromeo for her invaluable help in maintaining cell lines, preparing solutions, and other technical assistance, Dr. Jay Justice of Emory University for his advice on amperometry in the early stages of this work, and Dr. Julio Fernandez and members of his laboratory at the Mayo Foundation for expert guidance on the manufacture and use of low-noise microamperometric electrodes. This work was supported by a National Alliance for Research on Schizophrenia and Depression Young Investigator Award to A.G. and senior National Alliance for Research on Schizophrenia and Depression awards and National Institutes of Health Grants NS-34075 and NS-33373 to R.D.B. and L.J.D.

1. Trendelenburg, T. (1991) *Trends. Pharmacol. Sci.* **12,** 334–337.
2. Giros, B. & Caron, M. G. (1993) *Trends Pharmacol. Sci.* **14,** 43–49.
3. Amara, S. & Kuhar, M. J. (1993) *Annu. Rev. Neurosci.* **16,** 73–93.
4. Blakely, R. D., DeFelice, L. J. & Hartzell, H. C. (1994) *J. Exp. Biol.* **196,** 263–281.
5. Lester, H. A., Mager, S., Quick, M. W. & Corey, J. L. (1994) *Annu. Rev. Pharmacol. Toxicol.* **34,** 219–249.
6. Barker, E. L. & Blakely, R. D. (1995) *Psychopharmacology* **28,** 321–333.
7. Masihiko, T., Groshan, K., Blakely, R. D. & Richelson, E. (1997). *Eur. J. Pharmacol.* **340,** 249–258.
8. Giros, B., Jaber, M., Jones, S. R., Wightman, R. M. & Caron, M. G. (1996) *Nature (London)* **379,** 6–612.
9. Wall, S. C., Gu, H. & Rudnick, G. (1995) *Mol. Pharmacol.* **47,** 544–550.
10. Bönisch, H. & Harder, R. (1986) *Naunyn-Schmiedeberg's Arch. Pharmacol.* **334,** 403–411.
11. Rudnick, G. (1997) *Neurotransmitter Transporters: Structure, Function and Regulation* (Humana, Clifton, NJ) pp. 73–100.
12. Lester, H. A., Cao, Y. & Mager, S. (1996) *Neuron* **17,** 807–810.
13. Lin, F., Lester, H. A. & Mager, S. (1996) *Biophys. J.* **71,** 3126–3135.
14. Galli, A., DeFelice, L. J., Duke, B. J., Moore, K. R. & Blakely, R. (1995) *J. Exp. Biol.* **198,** 2197–2212.
15. Sonders, M. & Amara, S. G. (1996) *Curr. Opin. Neurobiol.* **6,** 294–302.
16. DeFelice, L. J. & Blakely, R. (1996) *Biophys. J.* **70,** 579–580.
17. Wadiche, J. I., Amara, S. G. & Kavanaugh, M. P. (1995) *Neuron* **15,** 721–728.
18. Larsson, H. P., Picaud, S. A., Werblin, F. S. & Lecar, H. (1996) *Biophys. J.* **70,** 733–742.
19. Galli, A., Petersen, C. I., deBlaquiere, M., Blakely, R. D. & DeFelice, L. J. (1997) *J. Neurosci.* **17,** 3401–3411.
20. Sonders, M. S., Zhu, S. J., Zahniser, N. R., Kavanaugh, M. P. & Amara, S. G. (1997) *J. Neurosci.* **17,** 960–974.
21. Galli, A., Blakely, R. D. & DeFelice, L. J. (1996) *Proc. Natl. Acad. Sci. USA* **93,** 8671–8676.
22. Qian. Y., Galli, A., Ramamoorthy, S., Risso, S., DeFelice, L. J. & Blakely, R. D. (1997) *J. Neurosci.* **17,** 45–57.
23. Zhu, S. J., Kavanaugh, M., Sonders, M. S., Amara, S. G. & Zahniser, N. R. (1997) *J. Pharmacol. Exp. Ther.* **282,** 1358–1365.
24. Schroeder T. J., Jankowski, A., Kawagoe, K. T. & Wightman, R. M. (1992) *Anal. Chem.* **64,** 3077–3083.
25. Alvarez de Toledo, G., Fernandez-Chacon, R. & Fernandez, J. M. (1993) *Nature (London)* **363,** 554–558.
26. Albillos A., Dernick, G., Horstmann, H., Almers, W., Alvarez de Toledo, G. & Lindau, M. (1997) *Nature (London)* **389,** 509–511.
27. Jones, S. R., Gainetdinov, R. P., Wightman, R. M. & Caron, M. C. (1998) *J. Neurosci.* **18,** 1979–1986.
28. Stamford, J. A. & Justice, J. B., Jr. (1996) *Anal. Chem.* **68,** 359A–363A.
29. Burnette, W. B., Baily, M. D., Kukoy, S., Blakely, R. D., Trowbridge, C. G. & Justice, J. B., Jr. (1996) *Anal. Chem.* **68,** 2932–2938.
30. Bunin, M. A. & Wightman, R. M. (1998) *J. Neurosci.* **18,** 4854–4860.
31. Wightman, R. M., Jankowski, J. A., Kennedy, R. T., Kawagoe, K. T., Schroeder, T. J., Leszczyszyn, D. J., Near, J. A., Diliberto, E. J. & Viveros, O. H. (1991) *Proc. Natl. Acad. Sci. USA* **88,** 10754–10758.
32. Chow, R. H., von Ruden, L. & Neher, E. (1992) *Nature (London)* **356,** 60–63.
33. Ciolkowski, E. D., Maness, K. M., Cahill, P. S. & Wightman, R. M. (1994) *Anal. Chem.* **66,** 3611–3617.
34. Pacholczyk, T. Blakely, R. D. & Amara, S. G. (1991) *Nature (London)* **350,** 350–354.
35. Ramamoorthy, S., Prasad, P. D., Kulanthaivel, P., Leiback, F. H, Blakely, R. D. & Ganapathy, V. (1993) *Biochemistry* **32,** 1346–1353.
36. Fisher, L. D. & van Belle, G. (1993) *Biostatistics* (Wiley, New York) Vol. 9, pp. 371–374.
37. Buck, K. J. & Amara, S. G. (1995) *Mol. Pharmacol.* **48,** 1030–1037.
38. Friedrich, U. & Bönisch, H. (1986) *Naunyn-Schmiedeberg's Arch. Pharmacol.* **333,** 246–252.
39. Gu, H. H., Wall, S. & Rudnick, G. (1996) *J. Biol. Chem.* **271,** 6911–6916.
40. Corey, J. L., Quick, M. W., Davidson, N. Lester, H. A. & Guastella, J. (1994) *Proc. Nat. Acad. Sci. USA* **91,** 1188–1192.
41. Cammack, J. N., Rakhilin, S. V. & Schwartz, E. A. (1994) *Neuron* **13,** 949–960.
42. Cammack, J. N. & Schwartz, E. A. (1996) *Proc. Natl. Acad. Sci. USA* **93,** 723–727.
43. Schroeder, T. J., Jankowski, A., Kawagoe, K. T. & Wightman, R. M. (1992) *Anal. Chem.* **64,** 3077–3083.
44. Perlman, R. L. & Sheard, B. E. (1982) *Biochim. Biophys. Acta* **719,** 334–340.
45. Olefirowicz, T. M. & Ewing, A. G. (1990) *Anal. Chem.* **62,** 1872–1876.
46. Zetterstrom, T., Sharp, T., Marsden, C. A. & Ungerstedt, U. (1983) *J. Neurochem.* **41,** 1769–1773.
47. Bert, R. F., Denoroy, L. & Renaud, B. (1995) *Anal. Chem.* **67,** 1838–1844.
48. Clements, J. D. (1996) *Trends Neurosci.* **19,** 163–171.